The marine atmospheric boundary layer over the eastern Pacific and its simulation in climate models

Michael A. Brunke[1], Xubin Zeng[1], and Mingyu Zhou[1,2]

[1]Department of Atmospheric Sciences, The University of Arizona, Tucson, Arizona

[2]National Research Center for Marine Environmental Forecasts, Beijing, China

Introduction

The marine atmospheric boundary layer (MABL) over the eastern Pacific is intimately connected to cloud processes in this region. Surface processes and cloud and convective processes are coupled through the MABL. Thus, it is important to have an accurate representation of both ABL and cloud properties in climate models.

In this paper, an analysis of almost 1000 soundings taken over the eastern Pacific is done to establish a climatology of *h* in this region which is compared to model results from NCAR's CCSM (Zeng et al. 2004) and NCEP's Climate Forecasting System (CFS). Some suggestions are made as to how to improve the formulation of *h* in these models. Furthermore, an analysis of field experimental data from over the eastern Pacific as well as other regions around the world has revealed the statistical characteristics of macro- and microphysical properties of stratus/stratocumulus such as cloud thickness, cloud base, cloud top, and cloud liquid water path (LWP) (Zhou et al. 2006). These results are expected to lead to an improvement of the treatment of stratus/stratocumulus clouds in numerical weather prediction and climate models.

Contact Information

Michael A. Brunke, Department of Atmospheric Sciences, The University of Arizona, 1118 E. 4th St., P. O. Box 210081, Tucson, AZ 85721-0081, e-mail: brunke@atmo.arizona.edu

Acknowledgments

This work was supported by NOAA (NA16GP1619 and NA050AR4310008) and NSF (ATM0301188). M. Zhou was also supported by NSFC (40233032 and 40075001) and MOST (2001DIA20026).

References

Considine, G., J. A. Curry, B. Wielicki, 1997: Modeling cloud fraction and horizontal variability in marine boundary layer cloud. *J. Geophys. Res.*, **102**, 13 517-13 525.

Vogelezang, D. H. P., and A. A. M. Holtslag, 1996: Evaluation and model impacts of alternative boundary-layer height formulations. *Bound.-Layer Meteor.*, **81**, 245-269.

Zeng, X., M. A. Brunke, M. Zhou, C. Fairall, N. A. Bond, and D. H. Lenschow, 2004: Marine atmospheric boundary layer height over the eastern Pacific: Data analysis and model evaluation. *J. Climate*, **17**, 4159-4170.

Zhou, M., X. Zeng, M. Brunke, Z. Zhang, and C. Fairall, 2006: An analysis of statistical characteristics of stratus and stratocumulus over eastern Pacific. *Geophys. Res. Letters*, in press.

The boundary layer height over the eastern Pacific

Data

The 973 soundings used to investigate *h* over the eastern tropical and subtropical Pacific Ocean were obtained from 11 cruises over the region from 1995 to 2001. These included radiosonde data from the Tropical Eastern Pacific Process Study (TEPPS) and the Eastern Pacific Investigation of Climate Processes in the Coupled Ocean-Atmosphere System (EPIC). The data were quality controlled. Poor or missing data were removed and filled in by linear interpolated values. Finally, the soundings were smoothed using a 1-2-1 smoother.

Marine ABL height determined from radiosonde data

ABL height was determined from the radiosonde data using a quantitative and objective criterion:

- For unstable ABL's, *h* is defined as the height starting near-surface where the vertical gradient of virtual potential temperature, $\partial\theta_v/\partial z$, first becomes greater than or equal to 3 K km^{-1}.
- For stable ABL's, *h* is define as the height from near-surface where the bulk Richardson number first becomes greater than 0.3 based on Vogelezang and Holtslag's (1996) criterion [see Eq. (1)].
- Finally, if *h* determined by either of the two formulations above happens to fall withing a cloud layer, then *h* is further adjusted based on the thickness of the cloud, *D*. If the cloud is thin ($h \geq D$), then *h* is taken as the cloud top. If the cloud is thick ($h < D$), then *h* is adjusted to the cloud base.

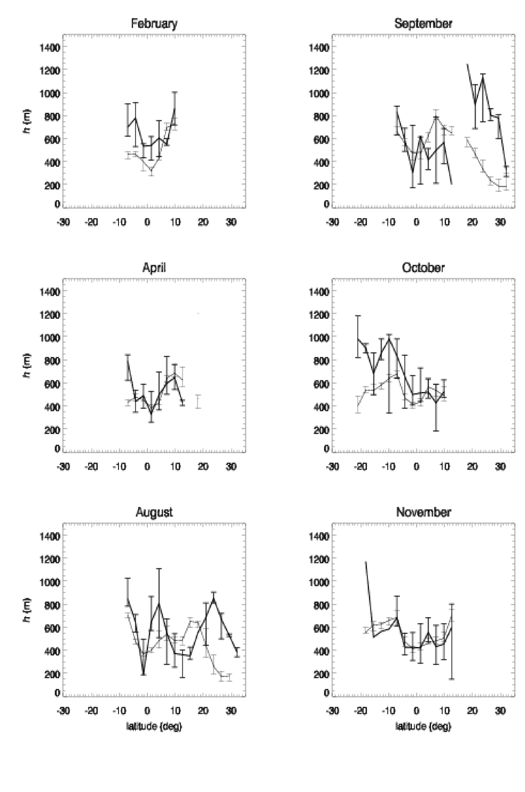

Fig. 1. The zonal median ABL height for each 2.8° latitude belt for *h* derived from soundings in the eastern Pacific using the above criterion (thick lines) as well as those from the CCSM control run (thin lines). Also shown are the interquartile ranges in each belt (the difference between the 25th and 75th percentiles, vertical lines).

- *h* is at its minimum in February, not varying much between 2.8°S and 8.4°N,
- There are three minima in *h* in August: near the Equator, in the ITCZ, and over the subtropical stratus/stratocumulus regime off of the Californian/Mexican coastlines.
- There are three maxima in *h* in August: over the stratocumulus region of the southeast Pacific, between the equator and the ITCZ, and around 24°N.

There are also meridional, seasonal, and interannual variability in *h*. For instance, the meridional variability in *h* is as large as the latitudinal variability. Also, the variation in *h* over a three-year period (1999-2001) was very small from 4.2°S to 1.4°S. Elsewhere, there could be a large variation in *h*.

Marine ABL heights from the CCSM

In the CCSM, *h* is determined as for stable conditions in our objective criterion in which *h* is defined as the height in which the bulk Richardson number,

$$Ri_b = \frac{\frac{g}{\theta_v(z_s)}(h-z_s)[\theta_v(h)-\theta_{vs}]}{[u(h)-u(z_s)]^2+[v(h)-v(z_s)]^2+\beta u_*^2} \quad (1)$$

where z_s is the height of the lowest model layer, θ_v is the virtual potential temperature, *u* and *v* are the horizontal wind components, u_* is the friction velocity, *g* is gravitational acceleration, and β is taken to be 100, is equal to a critical value of 0.3. It is used for both stable and unstable ABL's. So, under unstable conditions, the effect of convective updrafts is accounted for in the near-surface virtual potential temperature, θ_{vs}:

$$\theta_{vs} = \theta_v(z_s) + b\frac{(\overline{w'\theta_v'})_s}{w_m} \quad (2)$$

where *b* is taken to be 8.5; $(\overline{w'\theta_v'})_s$ is the surface buoyancy flux; and w_m is a velocity scale such that $w_m = (u_*^3 + 0.6 w_*^3)^{1/3}$, w_* being the convective velocity scale:

$$w_* = \left[\frac{g}{\theta_{v0}}(\overline{w'\theta_v'})_s h\right]^{1/3} \quad (3)$$

For the 100-year control run of the CCSM (version 2, thin lines in Fig. 1):

- The model produces results consistent with observed *h* in April and November.
- In February and October, there are some significant differences at the 95% level between the model and observed *h*.
- In August and September, CCSM *h* is significantly underestimated north of 20°N, and, while the model correctly produces a minimum *h* near the equator, it fails to produce one in the ITCZ.

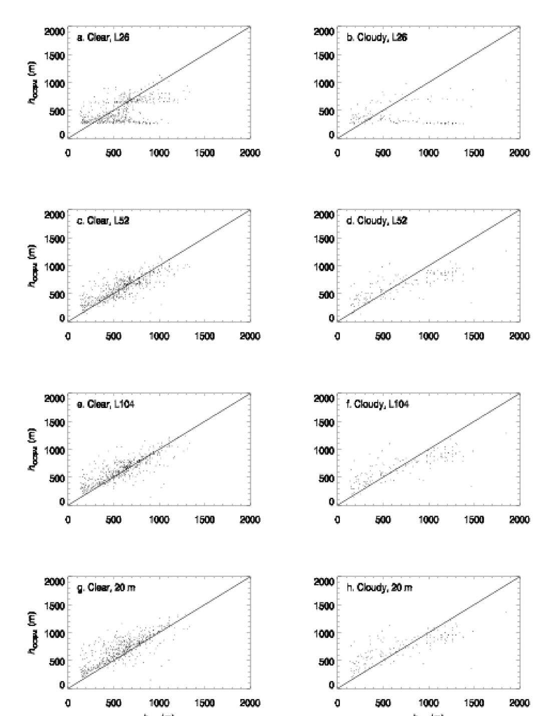

Fig. 2. Comparison of the ABL height using the CCSM formulation (h_{CCSM}) with that observed (h_{obs}) under (left) clear and (right) cloudy conditions, respectively, using (a), (b) the original vertical resolution of 26 layers (L26); (c), (d) doubling of the number of layers (L52); (e), (f) quadrupling of the number of layers (L104); and (g), (h) sounding data resolution (~20 m).

- Model *h* is greatly improved simply by doubling the number of model layers.
- Little or no improvement is made at L104 or 20 m resolution.
- A smaller improvement is made if *h* is further adjusted to account for the presence of a cloud layer if there is one.

Marine ABL heights from the CFS

CFS' formulation for the calculation of *h* is similar to CCSM's except that the bulk Richardson number is calculated from the surface not the lowest model layer, i.e.,

$$Ri_b = \frac{\frac{g}{\theta_v(z_s)}h[\theta_v(h)-\theta_{vs}]}{u(h)^2+v(h)^2} \quad (4)$$

and is set to a slightly higher critical value of 0.5 at *h*. Note that there is also no βu_*^2 term which takes into account wind gustiness effects. Also, *b* is taken to be 7.8.

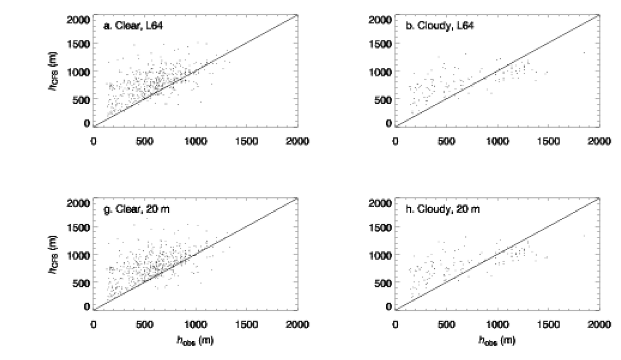

Fig. 3. Same as in Fig. 2 except for CFS using (a), (b) the model's vertical resolution of 64 layers (L64) and (c), (d) sounding data resolution.

- The model usually overpredicts *h*.
- No improvement is made when the vertical resolution is increased to 20 m.

Further sensitivity tests have shown that the probable culprits of this overprediction are the calculation of Ri_b from the surface rather than the first model layer and from the lack of a wind gustiness term.

Preliminary results of CCSM runs

We have run the atmospheric component of the CCSM coupled to its land component to see how a change in the calculation of *h* would affect model simulations. We have added an accounting for the existence of cloud layers when calculating *h* in the presence of oceanic stratus/stratocumulus. Preliminary results (Fig. 4) reveal that there are substantial differences even over land between a two-year run using that version compared to the control run.

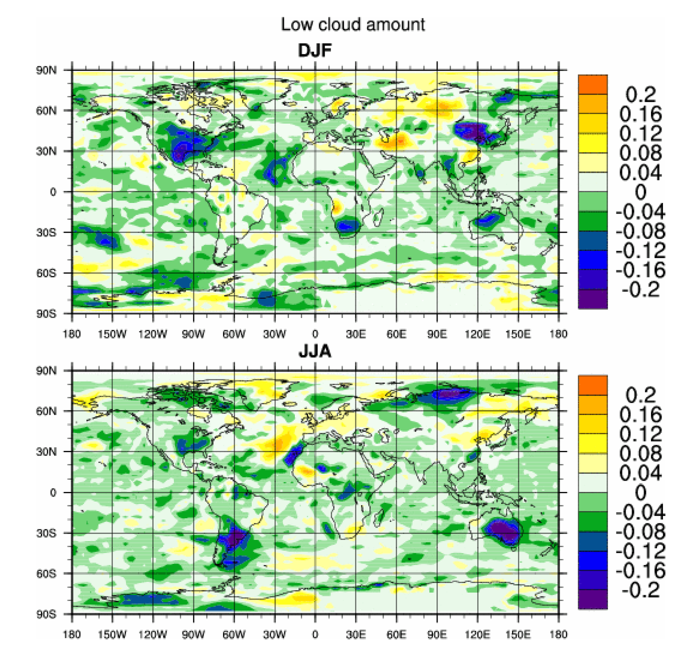

Fig. 4. The mean difference in low cloud amount between two model runs of the atmospheric component of CCSM coupled to the land component only, an experimental version which accounts for the presence of clouds when calculating *h* and a control version with no changes. Shown are the mean difference in winter (DJF, top) and summer (JJA, bottom).

Statistical characteristics of stratus and stratocumulus over the Eastern Pacific

Data

The data used here was mostly from the second half of the EPIC cruise in which the ship traversed the southeastern Pacific stratocumulus region. CF and cloud base, LWP, and cloud top were derived from measurements made by a ceilometer, a microwave radiometer, and cloud radar, respectively. To avoid the possible influence of continental contamination, we only used data from a five-day period (10-14 October 2001) in which there were complete measurements of CF, LWP, and cloud base and top heights.

Is LWC adiabatic?

To answer this, we consider LWP, which is the vertical integral of LWC over the cloud thickness, *D*:

$$LWP = \alpha\frac{A}{2}D^2 \quad (5)$$

where *A* is the adiabatic change of LWC with height and α is a constant describing the deviation from adiabatic LWC. Thus, if LWC was completely adiabatic, α would be 1. Previous studies have shown *A* to range from 2.0×10^{-3} to 2.8×10^{-3} g m^{-4}.

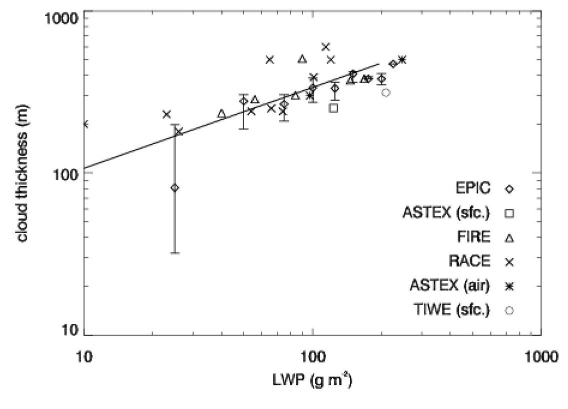

Fig. 5. The log-log relationship between cloud thickness and LWP in 25 g m^{-2} bins using surface and aircraft measurements over different oceanic regions. The vertical lines for EPIC are the IQR's of those bins. Also shown is the best fit to the EPIC data (solid line).

- The data in Fig. 5 shows that LWP is proportional to D^2 as described by Eq. (5).
- The value of αA derived from Fig. 4 is 1.76×10^{-3} g m^{-4}, which means that α would have to be 0.79 using the median value of *A* and varies between 0.68 and 0.84. This implies that the increase in LWC with height is about 21% less than the adiabatic value.

Are cloud properties normally distributed?

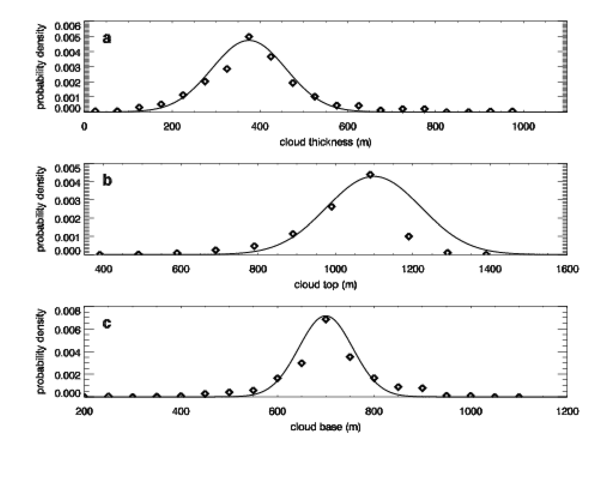

Fig. 6. Mean probability distribution functions of (a) cloud thickness, (b) cloud top height, and (c) cloud base height. Fits to normal distributions are shown as the solid lines.

- Cloud thickness and cloud base fit a normal distribution better than cloud top. These three distributions are statistically indistinguishable from normal distributions according to Kolmogorov-Smirnov significance testing, but the distribution of cloud top height is the least likely to be the same as a normal distribution.

Can we parameterize CF using LWP?

Such probability distributions can be used to develop a statistical model to calculate CF (e.g., Considine et al. 1997). In this type of model, CF is defined as the integral of the probability distribution of LWP, *p*(*LWP*), starting from a threshold of LWP in which air is defined to be cloudy, δ:

$$CF = \int_{\delta}^{\infty} p(LWP)\, d(LWP) \quad (6)$$

in which

$$p(LWP)\, d(LWP) = p(D)\, dD \quad (7)$$

From Fig. 6, *p*(*D*) can be assumed to have a normal distribution. So,

$$p(D) = \frac{1}{(2\pi)^{1/2}\sigma_D}\exp\left[\frac{-(D-\bar{D})^2}{2\sigma_D^2}\right] \quad (8)$$

where $\bar{D}$ and σ_D are the mean and standard deviation of cloud thickness respectively. From Eqs. (5), (7), and (8),

$$p(LWP) = \frac{[(2\alpha A\, LWP)^{1/2}]^{-1}}{(2\pi\sigma_D^2)^{1/2}}\exp\left\{\frac{-[(LWP)^{1/2}-(\overline{LWP}-[1/2]\alpha A\sigma_D^2)^{1/2}]^2}{\alpha A\sigma_D^2}\right\} \quad (9)$$

Furthermore, the relationship between σ_{LWP} and σ_D can be derived from Eq. (5):

$$\frac{\sigma_{LWP}}{\sigma_D} = (2\alpha A\, LWP)^{1/2} \quad (10)$$

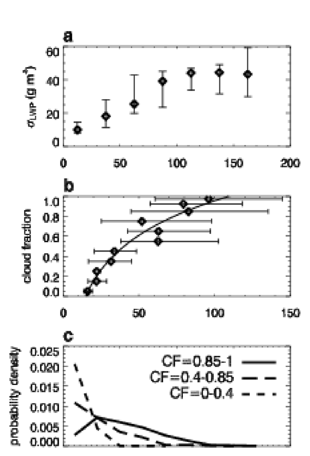

Fig. 7. (a) Relationship between σ_{LWP} and LWP in 25 g m^{-2} bins. (b) Relationship between LWP (in logarithmic scale) and CF in 0.1 bins with horizontal lines representing the IQR's and the other line denoting the fit to the data. (c) The probability distributions of LWP for different intervals of CF.

- If either σ_D or σ_{LWP} is known, than CF can be directly obtained from the integration of Eq. (6).
- Theoretically, CF could also be obtained through Eqs. (6), (9), and (10) and a relationship between σ_{LWP} and LWP. Fig. 7a shows such a relationship in which σ_{LWP} almost linearly increases with LWP for LWP less than 100 g m^{-2} and nearly constant for higher LWP.
- CF could be obtained through a direct relationship between CF and LWP derived from observational data. For EPIC, CF is shown to increase logarithmically with increasing LWP. However, there is large scattering for CF > 0.5. Fig. 7c shows *p*(*LWP*) for three different CF intervals during EPIC. For the highest CF (CF = 0.85-1), *p*(*LWP*) is lognormal. For the lowest CF (CF = 0-0.04), *p*(*LWP*) is close to exponential, whereas for CF = 0.4-0.85, the probability distribution is somewhere in between.

These results suggest that, while it is tempting to use simply LWP to find CF in numerical models, it is more appropriate to use different CF vs. LWP relations for various regimes or use a relationship between CF and relative humidity. A similar analysis of different relative humidity intervals should be undertaken to determine its relationship to CF.